

# Self-Mixing Laser Diode Velocimetry: Application to Vibration and Velocity Measurement

Lorenzo Scalise, Yanguang Yu, Guido Giuliani, *Member, IEEE*, Guy Plantier, *Member, IEEE*, and Thierry Bosch, *Member, IEEE*

**Abstract**—A review of recent experimental and theoretical results about laser diode self-mixing velocimetry is presented, showing that this technique can be deployed to measure velocity and vibration of solid targets with an extremely simple optical setup. This technique reduces optical alignment problems and achieves results comparable to those obtained by the conventional laser Doppler velocimetry (LDV) approach. It is demonstrated that the self-mixing signal can be processed to recover the target velocity and vibration by applying the same analysis method used for LDV. An optimal signal processing method is then proposed to recover the target velocity with good accuracy, also in the presence of relevant speckle disturbance. Application to the measurement of sub-micron vibrations is also demonstrated, using a self-mixing vibrometer instrument capable of 5-nm accuracy. As an example, the characterization of response and hysteresis of piezoceramic transducers (PZTs) is carried out. These results illustrate the effectiveness of the self-mixing technique in the field of laser velocimetry, opening the way to new applications where compactness and low cost of the measuring apparatus are essential.

**Index Terms**—Doppler frequency estimation, optical feedback interferometry, piezoceramics, self-mixing, speckle pattern, vibration and velocity measurement.

## I. INTRODUCTION

**L**ASER DOPPLER VELOCIMETRY (LDV) [1] and laser Doppler vibrometry [2] are well-known measurement techniques widely used for the precise remote measurement of the velocity of fluids, and for accurate measurement of the displacement, velocity and acceleration of solid objects. With these types of instruments, it is possible to measure the velocity and displacement of the target surface, simply by using a light beam. Desirable features like high sensitivity, high accuracy, and contactless operation have led to a large diffusion of these instruments. These instruments have been successfully applied to the fields of classical mechanics, modal analysis, on-line quality control, vibration analysis and medicine, with obvious advantages with respect to other “classical” sensors, such as

accelerometers. Examples of the application of laser sensors are reported in [2], [3]. Besides the clear advantages offered by LDV systems, some drawbacks have practically limited their field of application. The main drawbacks are large overall dimensions of the optical head, weight, the need for accurate optical alignment, and the high cost. The high cost is caused by the use of a large number of optical components (lenses, mirrors, beamsplitters, and even acoustooptic modulators) needed to build the conventional Mach–Zehnder or Michelson interferometer. For the above reasons, research efforts have been made in the attempt to increase the diffusion of laser techniques, by reducing system complexity and cost.

A great impact in this field can be brought about by development of the laser diode self-mixing (or optical feedback) interferometry technique that is capable of high performance with an extremely simple and inexpensive experimental setup. The self-mixing (SM) configuration is simply based on a diode laser, the focusing optics, and the target under test, without the need for additional optical components. In fact, when a small fraction of the light reflected or back-scattered by the target re-enters the LD cavity, the power emitted by the LD is amplitude modulated by an interferometric signal. It can be detected by the monitor photodiode included in the LD package, and suitably processed electronically to perform velocity, displacement, vibration and distance measurements [6]. The first example of velocity measurements performed through the SM effect in a gas laser was presented by Rudd [4], and more recently a breakthrough occurred as LDs were used instead of gas lasers. The SM effect in LDs has then been widely studied, both theoretically and practically. A wide range of applications have been proposed, including modal vibration analysis and velocimetry of both solids and fluids, with interesting applications to medical purposes for the latter [5]–[14].

This paper reviews some experimental and theoretical results about laser diode self-mixing velocimetry obtained from a collaboration between the authors’ four laboratories during the last two years. These include the basic analysis for velocity and vibration signals, an advanced signal processing technique for velocity signals in the presence of relevant speckle effects, and vibration measurements with very high accuracy. In Section II, it is demonstrated that self-mixing signal processing can be carried out similarly to conventional LDV techniques, in order to recover the velocity of a moving target with a rough surface in terms of the Doppler frequency (DF), or the vibration amplitude. Therefore, SM can be considered a valid alternative to the usual interferometric configurations used in commercial LDV instruments (Mach–Zehnder or Michelson), still allowing

Manuscript received April 7, 2003; revised August 15, 2003. This work was supported in part by the ICTP Program for Training and Research in Italian Laboratories, Trieste, Italy.

L. Scalise is with the Dipartimento di Meccanica, Università Politecnica delle Marche, Ancona, Italy (e-mail: l.scalise@mm.univpm.it).

Y. Yu is with Dipartimento di Elettronica, Università di Pavia, Pavia, Italy, on leave from the College of Information Engineering, Zhengzhou University, Zhengzhou, China.

G. Giuliani is with Dipartimento di Elettronica, Università di Pavia, Pavia, Italy (e-mail: guido.giuliani@unipv.it).

G. Plantier is with Ecole Supérieure d’Electronique de l’Ouest, Angers, France (e-mail: guy.platier@eseo.fr).

T. Bosch is with the ENSEEIHT-LEN7, Toulouse, France (e-mail: bosch@len7.enseeiht.fr).

Digital Object Identifier 10.1109/TIM.2003.822194

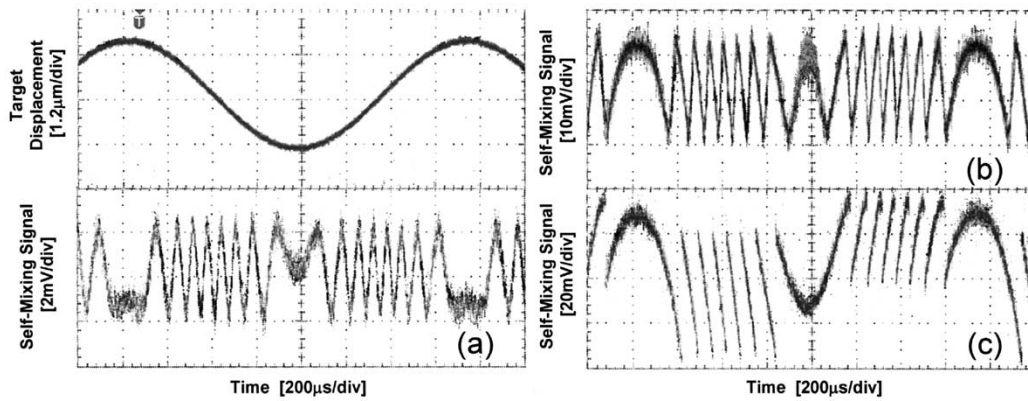


Fig. 1. Experimental SM signal interferometric waveforms obtained for different optical feedback regimes. The target is a loudspeaker. Upper-left trace: loudspeaker drive signal at 657 Hz,  $1.2 \mu\text{m}/\text{div}$ . (a) Very low feedback regime, external target reflectivity  $R_{\text{ext}} \approx 5 \cdot 10^{-9}$ ,  $C \ll 1$ ; the signal is a sine. (b) Low feedback regime,  $R_{\text{ext}} \approx 1.2 \cdot 10^{-7}$ ,  $C \approx 1$ ; the signal is a distorted sine. (c) Moderate feedback regime,  $R_{\text{ext}} \approx 2.5 \cdot 10^{-6}$ ,  $C > 1$ ; the signal is sawtooth-shaped and exhibits hysteresis.

the use of conventional DF processing units used for vibration analysis. Section III presents a new optimal signal processing method for the estimation of the Doppler frequency, and hence the target velocity, when multiplicative perturbations due to speckle effects are important. The method proposed is based on a new time series model of the self-mixing signal, which depends on the different parameters of the problem. This model is then used to not only estimate the DF with a maximum likelihood (ML) method, but also to find the theoretical Cramér–Rao lower bound (CRLB) for the estimation variance. Finally, Section IV reports on the application of the SM technique to the measurement of vibration waveforms with high accuracy. A suitably developed vibrometer instrument is used to carry out the characterization of the frequency response and hysteresis of piezoceramic transducers (PZTs).

The above results illustrate the effectiveness of the self-mixing technique in the field of laser velocimetry, opening the way to new applications where compactness and low cost of the measuring apparatus are essential.

#### A. Theory for Self-Mixing Interferometry

When a small fraction of the light back-reflected or back-scattered by a remote target re-enters into the laser cavity, a modulation of both the amplitude and the frequency of the lasing field is generated. The power emitted by the LD is amplitude-modulated by an interferometric waveform  $F(\phi)$  which is a periodic function of the back-injected field phase  $\phi = 2ks$ , where  $k = 2\pi/\lambda$  is the wavenumber and  $s$  is the distance from LD to target. The power emitted by the LD can be written as

$$P(\phi) = P_0 [1 + m \cdot F(\phi)] \quad (1)$$

where  $P_0$  is the power emitted by the unperturbed LD and  $m$  is a modulation index. The modulation index  $m$  and the shape of the interferometric function  $F(\phi)$  depend on the so-called feedback parameter  $C$  [6], [13]

$$C = \sqrt{R_{\text{ext}}} \cdot s_0 \cdot \frac{\varepsilon \sqrt{1 + \alpha^2}}{L_{\text{las}} n_{\text{las}}} \cdot \frac{1 - R_2}{\sqrt{R_2}} \quad (2)$$

where  $R_{\text{ext}}$  is target power reflectivity,  $\alpha$  (typ.  $\alpha = 3$ ) is LD linewidth enhancement factor,  $\varepsilon < 1$  (typ.  $\varepsilon = 0.5$ ) accounts for

a spatial mismatch between the reflected and the lasing optical modes,  $L_{\text{las}}$  is laser cavity length,  $n_{\text{las}}$  is cavity refractive index, and  $R_2$  is LD output facet power reflectivity. Thus, the value of the  $C$  parameter depends on both the amount of optical feedback and on the target distance  $s_0$ . The  $C$  parameter is of great importance, because it discriminates between different feedback regimes. For  $C \ll 1$  (weak feedback), the modulation index  $m$  is directly proportional to  $1/\sqrt{A}$ , and the function  $F(\phi)$  is a cosine, just like the usual interferometric waveform. When  $C$  approaches unity, the function  $F(\phi)$  resembles a distorted cosine, and its amplitude is still proportional to  $1/\sqrt{A}$ . For  $C > 1$  (moderate feedback regime, which corresponds to a target reflectivity of about  $10^{-5}$  for a target distance  $s_0 = 1$  m), the function  $F(\phi)$  becomes sawtooth-like and exhibits hysteresis. In this regime, the modulation coefficient  $m$  is around  $10^{-3}$  and it no longer increases for increasing target reflectivity. Examples of the experimental interferometric waveform obtained in the different feedback regimes are reported in Fig. 1. The maximum allowed target distance is limited to a few meters by the LD coherence length. When the target distance is comparable to the LD coherence length, the SM interferometric signal retains its shape, but the phase noise is increased [6].

## II. VELOCITY AND VIBRATION MEASUREMENT BY SELF-MIXING: LARGE VIBRATIONS

The sensor head used for the measurement of velocity for the case of large vibrations is simply composed by the LD and two focusing optics that realize the interferometer together with the target surface under test. The sensor layout of the self-mixing laser Doppler velocimeter is reported in Fig. 2. The packaged LD has 9 mm diameter, few millimeters of height, and few milligrams of weight. The used LD is a Philips CQL47A/D2, emitting at 825 nm with a maximum output power of 12 mW. The monitor photodiode (PD) included into the LD package acts as a transducer and it generates the SM ac current signal. The LD is driven by a constant current source. The optics used are Philips AO54,  $f = 4.4$  mm,  $\text{NA} = 0.46$ , and Olympus MD Plan X10,  $\text{NA} = 0.25$ . The Doppler frequency is measured by acquiring the SM signal with a 100-kHz spectrum analyzer (Ono Sokki, CF-5200). Time traces of the SM interferometric signal and its

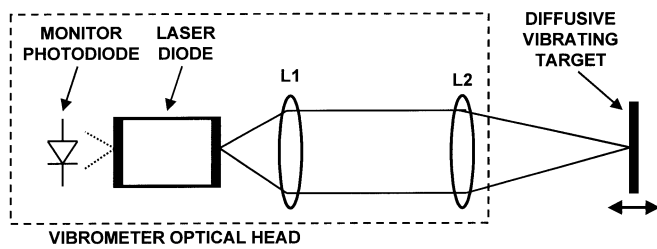


Fig. 2. Schematic of the SM sensor head composed by laser diode, internal monitor photodiode, and two discrete focusing optics.

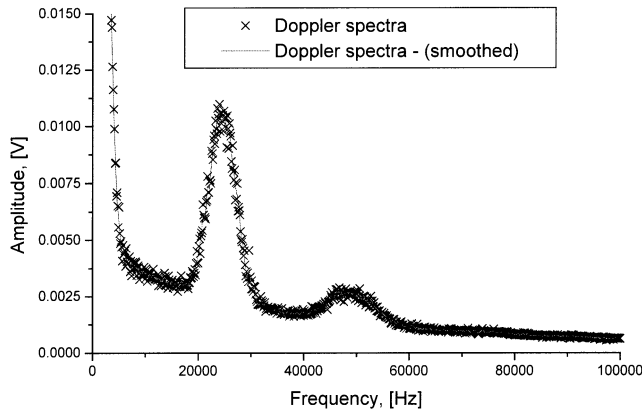


Fig. 3. Doppler signal generated from the SM laser Doppler velocimeter (x experimental values; FFT filter smoothing of experimental point. Smoothing is obtained using a seven-points adjacent averaging method).

power spectrum have been acquired and analyzed to extract the information relative to the velocity measurement. Fig. 3 reports the power spectrum of the self-mixing signal when the target is moving with a constant velocity. This is obtained using a rotating disc with white rough surface as a target, with a measurement angle between the optical axis of the sensor and the target surface of 30°. Rough data are reported together with smoothed data (a seven-point averaging algorithm is used). The theoretical relation for the Doppler Frequency  $F_D$  [1] is

$$F_D = \frac{2\nu \cos \theta}{\lambda} \quad (3)$$

where  $\nu$  is the modulus of the velocity vector,  $\theta$  is the angle between the optical axis of the sensor and the velocity vector, and  $\lambda$  is LD wavelength. The Doppler frequency of this signal is 24.3 kHz (corresponding to a target velocity of 11.6 mm/s). Fig. 4 reports the time trace of the self-mixing signal, where smoothed data have been obtained by filtering the rough data (low-pass filter with cut-off frequency of 1 MHz). By comparison with the traces of Fig. 1, it can be deduced that the system was operated in the moderate feedback regime, where the SM signal is sawtooth-like. This characteristic shape of the signal allows for easy discrimination of the target velocity sign [16]. This property of the self-mixing signals is extremely attractive, because it can help to massively reduce the complexity of the optical solutions used to discern the sign of the target velocity in conventional LDV systems, for which it is necessary to use a Bragg cell or opto-acoustic modulators.

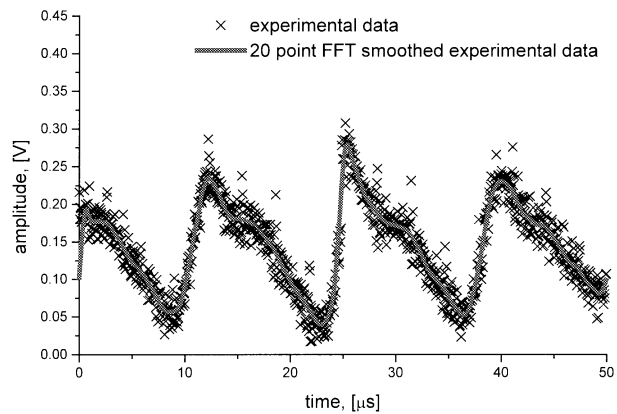


Fig. 4. Time trace of the SM signal for a velocity measurement performed on a white paper target surface moving toward the sensor. Smoothed trace is obtained using a software low-pass filter at 1 MHz.

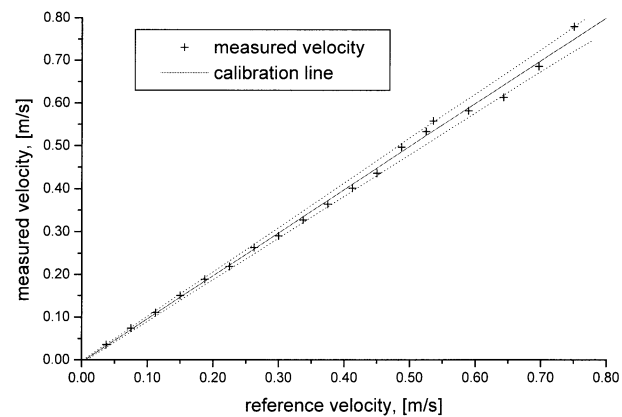


Fig. 5. Calibration of the SM velocity sensor (velocity range: 0–800 mm/s): experimental points and calibration line obtained as the best fitting of the experimental data (least-squares criterion). The  $\pm 3\sigma$  lines (repeatability below 3.5 %) are also shown.

Experimental values of the velocity of a reference sample in the range 0–800 mm/s, obtained using a 20 Hz–40 MHz spectrum analyzer (HP3585 A), have been compared with the DF values from (3), where values of  $\nu$ ,  $\theta$  and  $\lambda$  were firstly determined. Maximum inaccuracy between theoretical and experimental values of the DF was 8.5 % for a velocity value of 5 mm/s. For velocity values higher than 30 mm/s the inaccuracy is always lower than 4 % of the theoretical value. Accuracy is reduced as the angle  $\theta$  is increased, due to the reduction of the back-reflected radiation, which gives smaller signal-to-noise ratio, and also due to the increase of speckle effects [15].

Static characteristics of the sensor have been determined in the velocity range 0–800 mm/s. The calibration test bench [15] is realized by positioning the SM sensor in front of a white painted rotating wheel of about 30 cm of diameter, moved by an electric motor controlled by a stabilized power supply. Different velocity values in the range: 0–800 mm/s can be obtained by focusing the LD light along the rotating wheel radius at different distance from the rotation axis. Fig. 5 reports the calibration line obtained as the best fitting of the experimental data (least-squares criterion) and the  $\pm 3\sigma$  lines. Fig. 6 reports the variation of the Doppler peak as a function of the distance between the rotating surface and the sensor. The signal amplitude

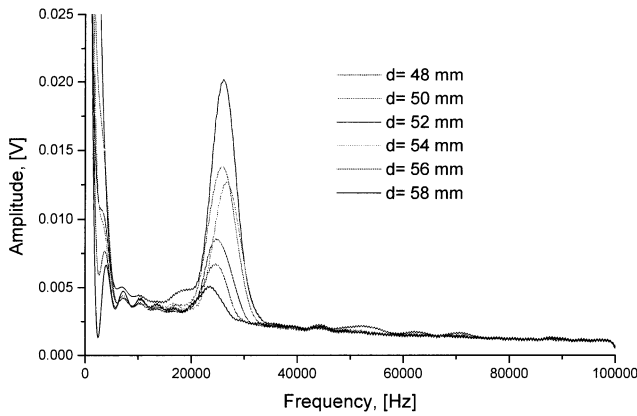


Fig. 6. Peak amplitude of the SM Doppler signal as a function of the target distance.

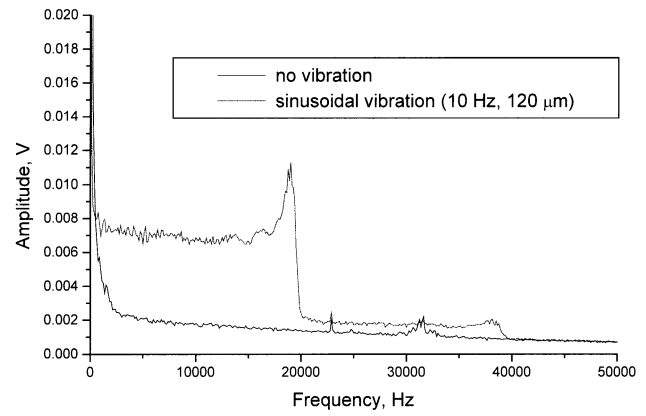


Fig. 8. Frequency spectra generated by the self-mixing sensor for a sinusoidally vibrating target (10 Hz frequency and 120  $\mu\text{m}$  amplitude).

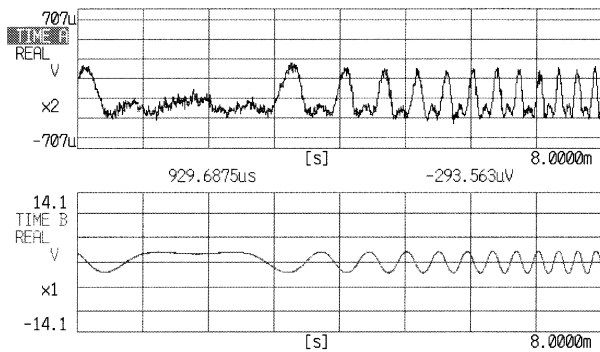


Fig. 7. Interference signals generated by the SM sensor (upper trace) and by the reference LDV (lower trace), for the case of a sinusoidally vibrating target. The same trigger signal is used for the two traces. A clear difference in the instantaneous frequency of the two signal can be observed, due to the different wavelengths of the lasers used (SM: 800 nm; reference: 632 nm).

depends on the arrangement used for the focusing system, and the maximum amplitude has been obtained for a distance of 52 mm, in this case.

A dynamic characterization of the SM sensor has been carried out utilizing a commercial LDV instrument for comparison (Ometron VS 100). The test bench was completed by an electrodynamic exciter (Bruel & Kjaer 4809) and by a spectrum analyzer (Ono Sokki, CF 5220). The electrodynamic shaker, used to generate a controlled vibrational behavior, has been driven by a power amplifier (Gearing & Watson SS30). Time signals generated by the SM sensor and by the Laser Doppler Vibrometer are reported in Fig. 7. It is possible to observe the inversion of the direction of motion of the target around the time coordinate of 1.8 ms. The power spectra of the SM interference signals for the cases of sinusoidal vibration of the target (10-Hz frequency and 120- $\mu\text{m}$  amplitude) and no vibration are reported in Fig. 8.

### III. OPTIMAL VELOCITY MEASUREMENT ALGORITHM

Low cost and contactless velocity measurements performed with LDs exploiting the self-mixing or optical feedback interferometry, have been studied in some research works [5], [17]–[19]. The principle of these measurement methods mainly consists in a precise estimation of the Doppler Frequency  $F_D$  from a spectral analysis of the SM signal  $v(t)$ . To reach this

goal, a digital signal processing is usually adopted, where  $v(t)$  is sampled at the sampling frequency  $F_e = 1/T_e$ , where  $T_e$  is the sampling time interval. A digital signal  $v(k) = v(kT_e)$  is obtained and subsequently processed to estimate  $F_D$ . Throughout the present analysis, the normalized frequency  $f_D = F_D/F_e$  is used, which represents the frequency as a fraction of the sampling frequency.

When a rough target backscatters the coherent light of the LD, the SM signal is corrupted by a multiplicative noise caused by the speckle effect [20] that causes random amplitude modulation of the signal, thus leading to the loss of the ideal sinusoidal waveform of the signal. Furthermore, a wide-band additive noise is often present in practical situations (i.e., photodetection shot noise). The presence of two types of noises (additive and multiplicative) make the estimation of the DF more difficult, so that suitable and efficient digital signal processing algorithms have to be developed.

Classical spectral analysis methods based on the use of a simple  $N$  points fast Fourier transform (FFT) of  $v(k)$  have been proposed in [12], [17], [18]. However, when the speckle effect is very strong, this technique gives unacceptably large DF estimations variances. Another technique proposed in [17] consists in performing an order 2 AutoRegressive (AR) spectral estimation of  $v(k)$ . This method has a very low algorithmic complexity and is therefore well adapted to real-time velocity measurement. Also, for speckle perturbations observed in a practical situation, estimation variances are much lower than the ones obtained with the simple FFT method. However, DF estimations obtained with this AR technique are biased if additive noise is important or if the DF greatly differs from the optimum value  $f_e/4$  [19].

#### A. Model for the Self-Mixing Signal

A model for the SM signal can be obtained from an analysis of its spectral properties. Fig. 9 shows a typical experimental time trace of  $v(t)$ , along with an estimation of its power spectral density (PSD) obtained with a simple averaged periodogram method [21]. This figure shows that the PSD can be modeled as a narrow band-pass signal centered on the DF, with a bandwidth dependent on the amount of the speckle effect: the more important the speckle effect, the larger the bandwidth. The SM signal  $v(k)$  can thus be considered as a wide sense stationary (WSS)

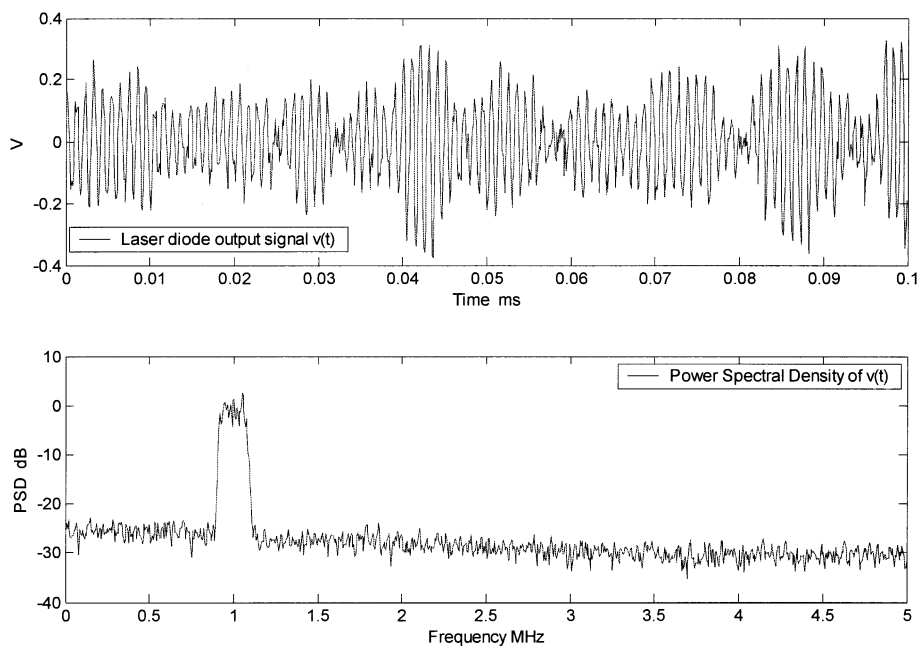


Fig. 9. Experimental velocity SM signal and its power spectral density, obtained for a constant target velocity.

Gaussian random process with a narrow bandpass PSD. As any WSS process,  $v(k)$  can always be modeled as the output of a linear shift invariant filter with a narrow band-pass frequency response  $H(f)$  excited at the input by a white noise  $x(k)$  with variance  $\sigma_x^2$  [21]. With these assumptions  $v(k)$  can be written as

$$v(k) = x(k) * h(k) + n(k) \quad (4)$$

where  $h(k)$  is the impulse response of the filter, the symbol  $*$  represents the convolution operator, and  $n(k)$  designates an additive white noise with variance  $\sigma_n^2$ .

To model the experimental PSD shown in Fig. 9 as closely as possible, a trapezoidal shape  $\Phi_v(f; \theta)$  has been chosen for the SM signal PSD, as illustrated in Fig. 10. In this model,  $f_m$  represents the half bandwidth of the process, and  $\varepsilon$  is the roll-off factor of the filter frequency response  $H(f)$ . From this PSD model, the signal-to-noise ratio (SNR) can be defined as the ratio of the narrow band-pass process power to the additive noise power

$$SNR = \frac{\sigma_x^2(4f_m + 2\varepsilon)}{\sigma_n^2}. \quad (5)$$

The notation used for the PSD shows that  $\Phi_v(f; \theta)$  depends on a vector of five unknown parameters  $\theta = [f_D, f_m, \varepsilon, \sigma_n^2, SNR]^T$  which have to be estimated, and where the superscript  $T$  denotes transposition. This estimation can be carried out using the ML method, by taking  $N$  samples of  $v(k)$  at successive times to generate the vector  $v_{0:N-1} = [v(0), v(1), \dots, v(N-1)]^T$ . Then, assuming that  $v(k)$  is a zero mean WSS Gaussian random process, the joint probability density function (PDF) of  $v_{0:N-1}$  is given by [22]

$$p(v_{0:N-1}; \theta) = \frac{1}{(2\pi)^{\frac{1}{2}} \{\det[C(\theta)]\}^{\frac{1}{2}}} \times \exp \left[ -\frac{1}{2} v_{0:N-1}^T C^{-1}(\theta) v_{0:N-1} \right] \quad (6)$$

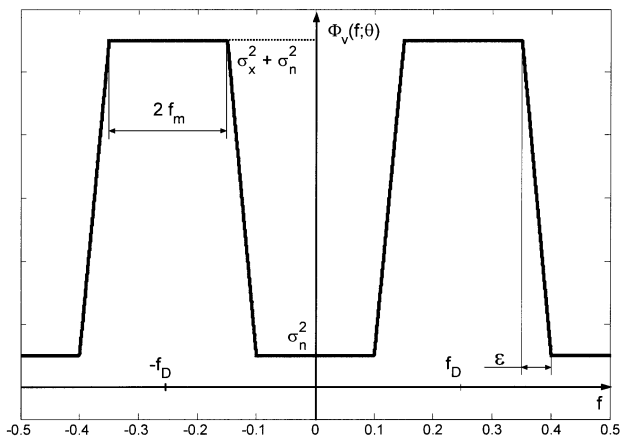


Fig. 10. Model of the SM signal power spectral density for a constant target velocity.

where  $C(\theta)$  is the  $N \times N$  covariance matrix of the process  $v(k)$ . This Toeplitz matrix takes on the form

$$c(\theta) = \begin{bmatrix} r_v(0; \theta) r_v(1; \theta) & \dots & r_v(N-1; \theta) \\ r_v(1; \theta) r_v(0; \theta) & \dots & r_v(N-2; \theta) \\ \dots & \dots & \dots \\ r_v(N-1; \theta) r_v(N-2; \theta) & \dots & r_v(0; \theta) \end{bmatrix} \quad (7)$$

where  $r_v(k; \theta)$  represents the autocorrelation function of  $v(k)$  given by the inverse Fourier transform of  $\Phi_v(f; \theta)$

$$r_v(k; \theta) = \sigma_x^2(4f_m + 2\varepsilon) \text{sinc}[(2f_m + \varepsilon)k] \times \text{sinc}(\varepsilon k) \cos(2\pi f_D k) + \sigma_n^2 \delta(k) \quad (8)$$

where  $\delta(k)$  is the Dirac function.

### B. Cramér–Rao Lower Bounds

In estimation theory, it can be shown that the variance of any unbiased estimator is bounded from below by the Cramér–Rao

bounds, which are computed from the PDF of  $v_{0:N-1}$ . For the  $5 \times 1$  vector parameter  $\theta$ , the CRLB asserts that the covariance matrix of an estimated vector  $\hat{\theta}$ , which is denoted  $C_{\hat{\theta}}$ , is always “larger” than the inverse of the positive semidefinite Fisher information matrix  $I_{\theta}$  [22]. In particular, this important result shows that the diagonal elements of  $C_{\hat{\theta}}$  and  $I_{\theta}^{-1}$  give a lower bound for the unknown parameters variances. For an estimated Doppler frequency  $\hat{f}_D$ , which is the first element of  $\hat{\theta}$ , we obtain

$$\text{Var}(\hat{f}_D) \geq [I_{\theta}^{-1}]_{1,1} \quad (9)$$

where  $[I_{\theta}^{-1}]_{i,j}$  denotes the  $[i,j]$  element of  $I_{\theta}^{-1}$  ( $i, j = 1, 2, \dots, 5$ ). For the WSS zero mean Gaussian process  $v(k)$ , we have [22]

$$[I_{\theta}]_{i,j} = \frac{1}{2} \text{tr} \left[ C^{-1}(\theta) \frac{\partial C(\theta)}{\partial \theta_i} C^{-1}(\theta) \frac{\partial C(\theta)}{\partial \theta_j} \right] \quad (10)$$

where  $\text{Tr}$  denotes the trace operator. The Doppler frequency variance computed directly from (9) and (10) is difficult to obtain analytically because of the requirement to invert the covariance matrix  $C(\theta)$ , and in general one shall perform a computer evaluation. However, for a large data record length  $N$ , an approximate asymptotic expression may be used, especially for the case of the WSS process  $v(k)$ . This asymptotic CRLB (ACRLB), which depends on the PSD  $\Phi_v(f; \theta)$ , is given by [22]

$$[I_{\theta}]_{i,j} = \frac{N}{2} \int_{-0.5}^{0.5} \frac{\partial \ln \Phi_v(f; \theta)}{\partial \theta_i} \cdot \frac{\partial \ln \Phi_v(f; \theta)}{\partial \theta_j} df \quad (11)$$

with large  $N$

Introducing in this expression the theoretical PSD  $\Phi_v(f; \theta)$  defined in Fig. 10, we obtain, after some straightforward calculations, an approximate asymptotic analytical CRLB for  $\hat{f}_D$ , which is noted ACRLB:

$$\text{Var}(\hat{f}_D) \geq \text{CRLB} \approx \text{ACRLB} = \frac{(2f_m + 1)\varepsilon}{N \times \text{SNR}}. \quad (12)$$

This result shows that the smaller the roll-off parameter  $\varepsilon$ , the smaller the theoretical variance. Furthermore,  $\text{Var}(\hat{f}_D)$  is independent of the Doppler frequency.

### C. Maximum Likelihood Doppler Frequency Estimation

The ML estimation method is very general and has the asymptotic properties of being unbiased and being able to achieve the CRLB [22]. The ML estimation  $\hat{\theta}$  is defined as the value of the vector parameter  $\theta$  that maximizes the PDF (6) [or the logarithm of (6)], when an  $N$  points experimental data record of  $v(k)$  is used for  $v_{0:N-1}$ . However, the ML estimation of  $\theta$  is difficult to obtain due to the need to invert a large dimension ( $N \times N$ ) covariance matrix  $C(\theta)$  and to maximize the highly nonlinear likelihood function (6). Fortunately, for a large data record of the WSS process  $v(k)$ , an asymptotic

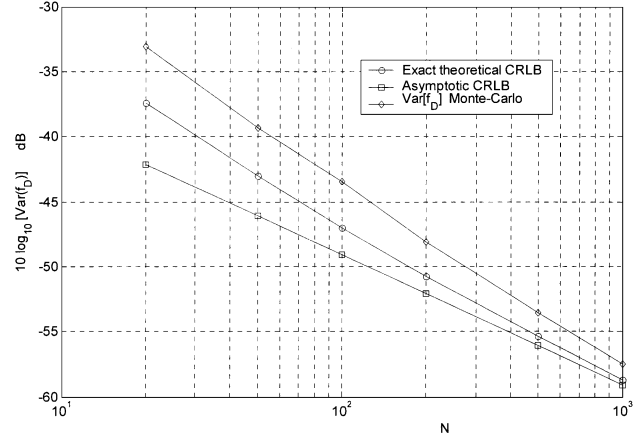


Fig. 11. Exact and asymptotic Cramér–Rao lower bound (CRLB) for the Doppler Frequency variance  $\text{Var}(\hat{f}_D)$  as a function of the number of samples  $N$ . A Monte-Carlo estimation of the asymptotic Maximum Likelihood variance is also plotted for comparison. Parameters values:  $F_D = 0.2$ ,  $f_m = 0.01$ ,  $\text{SNR} = 10$  dB,  $\varepsilon = 0.1$ .

expression of the log-likelihood function  $p$  can be used. This expression depends on the PSD  $\Phi_v(f; \theta)$  and is given by [22]

$$\ln [p(v_{0:N-1}; \theta)] \approx -\frac{N}{2} \ln(2\pi) - \frac{N}{2} \int_{-0.5}^{0.5} \left[ \ln \Phi_v(f; \theta) + \frac{P(f; N)}{\Phi_v(f; \theta)} \right] df \quad (13)$$

where  $P(f; N)$  represents the PSD estimation of  $v(k)$  obtained with the periodogram method, and it is defined as

$$P(f; N) = \frac{1}{N} \left| \sum_{k=0}^{N-1} v(k) \exp(-j2\pi f k) \right|^2.$$

The above expression can be efficiently computed with an FFT algorithm. Numerical maximization of (13) is simple and can be accomplished with iterative maximization procedures such as, for example, the Newton–Raphson method [23]. Such optimal algorithm has been implemented on a specialized digital processing hardware using a digital signal processor (DSP). The performance obtained shows that the simplified maximum likelihood method can be used for precise real time estimations of velocity, as required by many practical situations.

### D. Results

To illustrate the global performance of the methods presented in the previous sections, intensive Monte–Carlo simulations have been carried out with synthetic signal  $v(k)$  obtained from (4) as well as experimental measurements of the SM signal taken with a constant target velocity. Fig. 11 shows a comparison between the Doppler frequency variance obtained using the CRLB and the ACRLB for the following set of parameters  $f_D = 0.2$ ,  $f_m = 0.01$ ,  $\text{SNR} = 10$  dB and  $\varepsilon = 0.1$ . With these parameters, Monte-Carlo simulations using the asymptotic ML method give experimental variances greater than the theoretical CRLB by only 2 dB  $N \geq 200$ . Furthermore, the simple ACRLB given by (12) slightly underestimates the CRLB, but it gives

a very interesting insight of the ML method performances. Fig. 11 shows that, for practical values of the set of parameters, the standard deviation of the normalized Doppler Frequency for  $N = 1000$  is about  $10^{-3}$ . This corresponds to a relative accuracy of 0.5% on the Doppler Frequency. Furthermore, the obtained bias is very small, and it is in any case smaller than 0.1% of the DF. As the velocity is directly proportional to the Doppler frequency [see (3)], the above relative accuracy is also valid for the velocity.

#### IV. MEASUREMENT OF SUB-MICROMETER VIBRATIONS: CHARACTERIZATION OF PZT TRANSDUCERS BY THE SELF-MIXING VIBROMETER

In previous works, the self-mixing signal has been suitably processed to recover the displacement or vibration of a remote target when vibration amplitude is much larger than  $\lambda/2$  [12], [13], [15]; in addition, special techniques can be devised to achieve a resolution better than  $\lambda/2$  [24]. However, some applications require contactless measurement of vibrations with amplitude much smaller than the wavelength, and resolution in the nanometer range. These applications include characterization and analysis of piezoelectric transducers (PZTs), loudspeakers, and microelectromechanical systems (MEMS). To further extend the capabilities of the self-mixing technique toward these applications, a suitably designed vibrometer instrument has been realized by the Optoelectronic Group of the University of Pavia [25]. This vibrometer retains all the advantages of the self-mixing configuration (i.e., simplicity, compactness, low cost, ease of alignment), and it offers performances comparable to those obtained by conventional LDV instruments.

The main objective that led the development of the self-mixing laser vibrometer was the realization of an instrument capable of linearly transducing target vibrations into an electrical signal, so that resolution and sensitivity were limited by intrinsic photodetection noise and not by the quantization imposed by fringe-counting methods. The principle is based on a self-mixing interferometer operated in the moderate optical feedback regime (i.e., sawtooth-like interferometric signal), and on an electronic feedback loop that acts on LD injected current to achieve wavelength modulation. The interferometric phase is locked to the half-fringe position, and an active phase-nulling technique allows obtaining a wide dynamic range. The prototype version of the instrument is capable of linearly transducing vibrations of nearly all rough diffusive surfaces in a 0.1 Hz–70 kHz frequency range (only limited by the cut-off frequency of electronics, based on conventional operational amplifiers). It has a noise floor of 100 pm/ $\sqrt{\text{Hz}}$ , and a maximum dynamics corresponding to 200  $\mu\text{m}$  peak-to-peak amplitude [25]. The vibrometer is composed of an electronic unit and an optical head, shown in Fig. 2, which contains a 800 nm Fabry–Perot LD with monitor photodiode, a first collimating lens L1, and a second lens L2 that is used to focus the light onto the target. For the present application, the focal length of L2 is 7.5 cm. An electronic feedback loop (a schematic diagram of which is depicted in Fig. 12) detects the power variations caused in the self-mixing signal by the

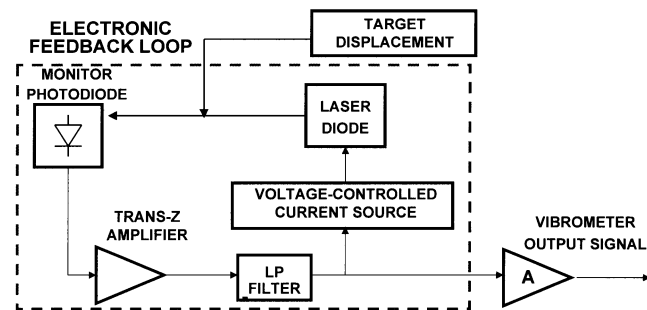


Fig. 12. Basic block scheme of the electronic feedback loop of the self-mixing laser vibrometer.

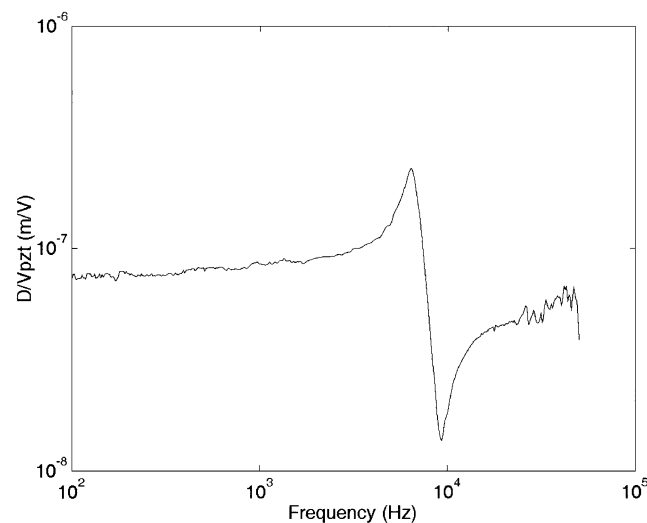


Fig. 13. Measured response for the stacked PZT transducer.  $D$  = displacement measured by the vibrometer;  $V_{\text{pzt}}$  = PZT drive voltage amplitude (equal to 10 V peak-to-peak at low frequencies). Swept-sine measurement is averaged over 100 cycles for each frequency step.

target displacement. It subsequently acts on the current injected into the LD with a proportional variation, so that the interferometric phase change caused by the wavelength modulation exactly compensates for the phase change caused by target displacement. An additional compensation path (not shown in Fig. 12) is used to cancel out the unwanted contribution of the LD output power modulation as the injection current is varied. The electrical signal supplied to the LD current driver, suitably amplified, represents the instrument output, with a responsivity of 10 mV/ $\mu\text{m}$ .

##### A. Application to PZT Transducers Characterization

The self-mixing laser vibrometer allows the measurement of very small vibrations with sub- $\mu\text{m}$  amplitude and moderate amplitude vibrations (i.e., in the  $\mu\text{m}$  range) with very high resolution (i.e., in the nanometer range). An application example that conveniently exploits the above characteristics is the experimental characterization of piezoceramic transducers (PZTs). Laser interferometry has been widely employed to characterize PZTs [26], [27], using conventional methods based on a He-Ne laser and Michelson or Mach–Zehnder interferometric configurations, which require a complicated experimental setup. The

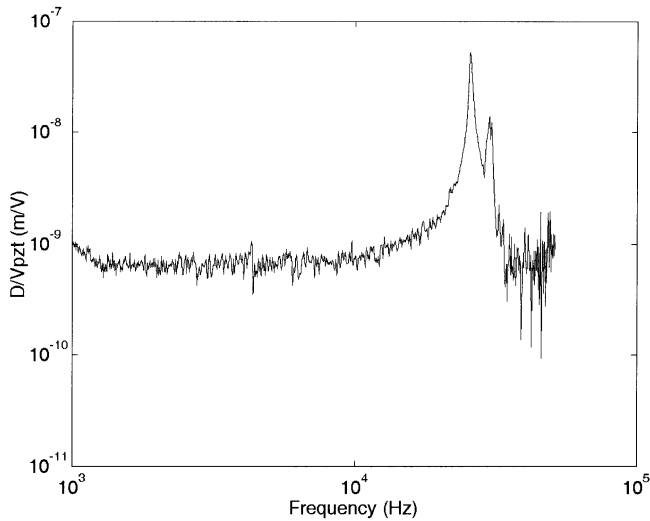
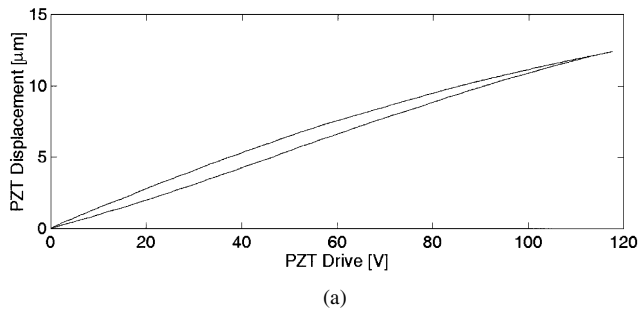
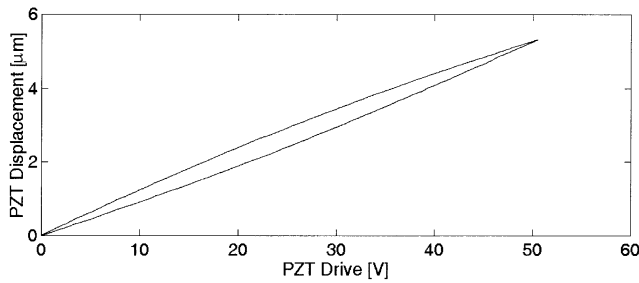


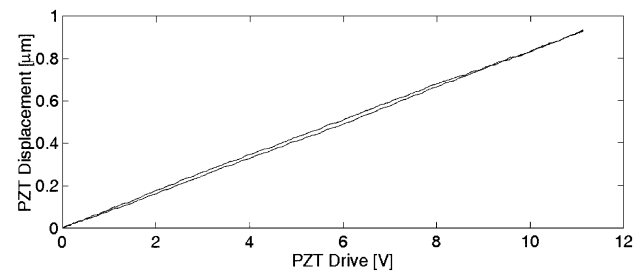
Fig. 14. Measured response for the cylinder PZT.  $D$  = radial displacement measured by the vibrometer;  $V_{pzt}$  = PZT drive voltage amplitude (equal to 20-V peak-to-peak at low frequencies). Swept-sine measurement is averaged over 100 cycles for each frequency step.



(a)



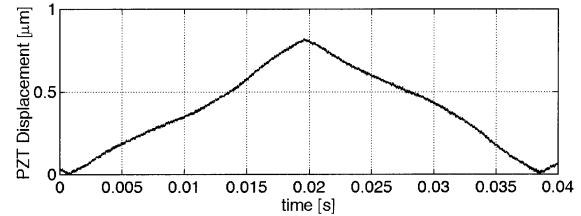
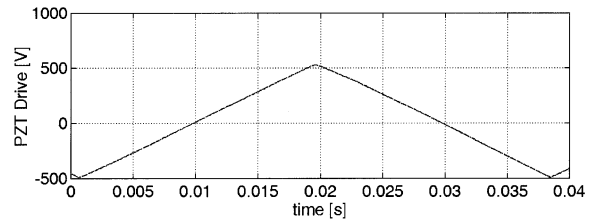
(b)



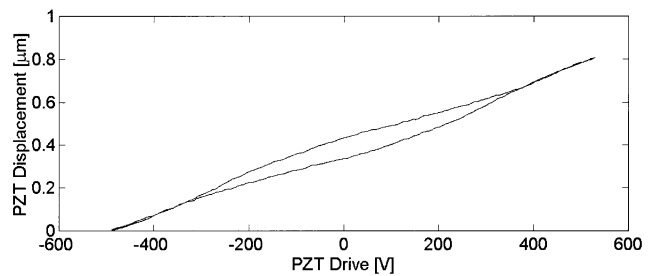
(c)

Fig. 15. Measured hysteresis loops for the stacked PZT. Drive voltage is 5-Hz sine. (a) PZT drive voltage amplitude = 118 V; (b) PZT drive voltage amplitude = 50 V; (c) PZT drive voltage amplitude = 11.5 V. Traces contain 10 000 points; they are averaged over 16 single-shot acquisitions by digital oscilloscope, and subsequently smoothed by 50 points average.

present work illustrates that a simple, rugged, portable instrument based on the self-mixing interferometric configuration can be successfully used to test PZTs.



(a)



(b)

Fig. 16. Measured hysteresis loop for cylinder PZT. Drive voltage is 26 Hz triangle wave with 1000 V amplitude. (a) Time domain traces: upper trace, drive voltage; lower trace, PZT displacement as measured by the self-mixing vibrometer. (b) Hysteresis loop. Traces contain 10 000 points; they are averaged over 16 single-shot acquisitions by digital oscilloscope, and subsequently smoothed by 50 points average.

Two types of PZTs are considered: a stacked PZT (PI P802.10) and a cylinder PZT (PZT5A material; internal diameter = 27.5 mm; external diameter = 34.6 mm; height = 22.4 mm). Two types of measurements are performed on each sample: a characterization of the PZT frequency response with a small applied drive voltage signal and the measurement of hysteresis cycles obtained by applying large voltage periodic drives. In the first measurement, the high sensitivity (i.e., low noise floor) of the self-mixing vibrometer is exploited, while in the second measurement extended dynamic range as well as high resolution are demonstrated. The PZT is placed at 7.5-cm distance from the optical head of the laser vibrometer, and its surface is left untreated. The PZT is driven by a power buffer amplifier, especially required by the stacked PZT due to its large electrical capacitance. A Hewlett Packard HP35665A Dynamic Signal Analyzer is used to perform swept-sine response analysis. Results of the frequency response measurement for the stacked PZT transducer are reported in Fig. 13, showing the ratio of the measured displacement  $D$  and the applied drive voltage  $V_{pzt}$ . A value  $D/V_{pzt} = 7.6 \cdot 10^{-8}$  m/V is found at low frequency, and resonant and anti-resonant frequencies are found respectively as 6.33 kHz and 9.05 kHz. In this measurement, the peak-to-peak value for  $V_{pzt}$  is 10 V, so that at low frequencies a displacement  $D \approx 800$  nm is generated. Fig. 14 reports the result for the radial displacement  $D$  of the cylinder PZT. A value  $D/V_{pzt} = 7 \cdot 10^{-10}$  m/V is found at

low frequencies, in good agreement with data reported in [28]. In addition, two resonances are found at 25.5 kHz and 30.0 kHz. In this measurement, the peak-to-peak value for  $V_{\text{pzt}}$  is 20 V, and at low frequencies a displacement  $D \approx 14$  nm is generated. The self-mixing vibrometer exhibits a good accuracy even for small vibration amplitudes, and it should be kept in mind that the data displayed in Fig. 14 are not smoothed nor post-processed.

To determine the dynamic hysteresis characteristic of the PZTs, a periodic voltage drive signal has been applied. The drive and displacement traces are simultaneously acquired by a digital oscilloscope, and the hysteresis loop is plotted using a PC. Hysteresis loops obtained for the stacked PZT for drive voltage amplitudes of 118 V, 50 V, and 11.5 V are reported in Fig. 15. Oscilloscope traces are averaged over 16 acquisitions, and further smoothing is performed by post-processing using a PC. Hysteresis width is around 10% of maximum displacement for 118 V and 50 V cases, and it is around 2.5% for the 11.5 V drive. The latter case is interesting to analyze the performance of the self-mixing vibrometer for a displacement smaller than  $1 \mu\text{m}$ ; it can be concluded that the accuracy attained for periodic time domain analysis is better than 5 nm. Fig. 16(a) and (16b) report time-domain traces and the hysteresis loop for the cylinder PZT driven by a triangular wave of 1000 V amplitude and 26 Hz frequency.

## V. CONCLUSION

This paper has reported on different aspects and applications of the self-mixing laser diode velocimetry/vibrometry technique, illustrating recent results obtained by Authors' research groups.

First, it has been illustrated that the self-mixing effect can be used to design and realize a laser Doppler velocimeter. Small dimensions, low weight and low costs are the main characteristics of this velocity sensor. Experimental results for the static and dynamic calibration of the sensor have been reported. The comparison with a commercial system has shown a coincidence of the performances, in terms of the maximum vibrational velocity measured.

A new model and a suitable processing algorithm for the analysis of self-mixing signal for velocity measurement have been developed for the case of relevant speckle effects. The SM signal is modeled as a wide sense stationary Gaussian random process with a narrow band-pass power spectral density, depending on a set of unknown parameters that have to be estimated. For this purpose, an optimal ML approach has been proposed to reduce as much as possible the variances of the Doppler Frequency estimations. A simplified version of this technique is also given and is shown to attain the minimal variance of any Doppler Frequency estimator given by the CRLB. Even for the case of large perturbations caused by the speckle effect, bias and standard deviations of about 0.5% of the velocity have been obtained. Therefore, the ML method seems to be a good solution to carry out the real-time signal processing required by a precise sensor for velocity measurements.

Finally, it has been demonstrated that a laser vibrometer based on the self-mixing scheme is capable of accurate measurements

of displacements with wide dynamic range and high accuracy. Application to PZT characterization is demonstrated for both frequency response and hysteresis measurements. In particular, hysteresis measurement by the SM technique is a very accurate method that offers great advantages over the all-electrical technique or capacitive displacement measurement.

## ACKNOWLEDGMENT

The authors would like to thank Prof. S. Donati, Prof. E. Primo Tomasini, and Prof. N. Paone for useful discussions.

## REFERENCES

- [1] L. E. Drain, *The Laser Doppler Technique*. Chichester, U.K.: Wiley, 1980.
- [2] P. Castellini, G. M. Revel, and E. P. Tomasini, "Laser Doppler vibrometry: a review of advances and applications," *The Shock Vib. Dig.*, vol. 30, no. 6, pp. 443–456, 1998.
- [3] E. P. Tomasini, G. M. Revel, and P. Castellini, "Laser based measurement," in *Encyclopaedia of Vibration*. London, U.K.: Academic, 2001, pp. 699–710.
- [4] M. J. Rudd, "A laser Doppler velocimeter employing the laser as a mixer-oscillator," *J. Phys. E*, vol. 1, pp. 723–726, 1968.
- [5] P. J. de Groot, G. M. Gallatin, and S. H. Macomber, "Ranging and velocimetry signal generation in a backscatter-modulated laser diode," *Appl. Opt.*, vol. 27, no. 21, pp. 4475–4480, November 1988.
- [6] G. Giuliani, M. Norgia, S. Donati, and T. Bosch, "Laser diode self-mixing technique for sensing applications," *J. Opt. A: Pure Appl. Opt.*, vol. 4, no. 6, pp. S283–S294, 2002.
- [7] M. K. Koelink, M. Slot, F. F. de Mul, and J. Greve *et al.*, "Laser Doppler velocimeter based on the self-mixing effect in a fiber-coupled semiconductor laser: theory," *Appl. Opt.*, vol. 31, pp. 3401–3408, 1992.
- [8] F. de Mul, L. Scalise, A. Petoukhova, M. van Herwijnen, P. Moes, and W. Steenbergen, "Glass-fiber self-mixing intra-arterial laser Doppler velocimetry: signal stability and feedback analysis," *Appl. Opt.*, vol. 41, no. 4, pp. 658–667, 2002.
- [9] M. K. Koelink, F. F. de Mul, A. L. Weijers, J. Greve, R. Graaff, A. C. M. Dassel, and J. G. Aarnoudse, "Fiber-coupled self-mixing diode laser Doppler velocimetry: technical aspects and flow velocity profile disturbance in water and blood flow," *Appl. Opt.*, vol. 33, pp. 5628–5641, 1995.
- [10] L. Scalise, W. Steenbergen, and F. de Mul, "Self-mixing feedback in a laser diode for intra-arterial optical blood velocimetry," *Appl. Opt.*, vol. 40, no. 25, pp. 4608–4615, 2001.
- [11] K. Meigas, H. Hinrius, R. Kattai, and J. Lass, "Self-mixing in a diode laser as a method for cardiovascular diagnostics," *J. Biomed. Opt.*, vol. 8, no. 1, pp. 152–160, 2003.
- [12] T. Bosch, N. Servagent, and S. Donati, "Optical feedback interferometry for sensing application," *Opt. Eng.*, vol. 40, no. 1, pp. 20–27, 2001.
- [13] S. Donati, G. Giuliani, and S. Merlo, "Laser diode feedback interferometer for measurement of displacements without ambiguity," *IEEE J. Quantum Electron.*, vol. 31, no. 1, pp. 113–119, 1995.
- [14] F. Gouaux, N. Servagent, and T. Bosch, "Absolute distance measurement with an optical feedback interferometer," *Appl. Opt.*, vol. 37, pp. 6684–6689, 1998.
- [15] L. Scalise and N. Paone, "Laser Doppler vibrometry based on self-mixing effect," *Opt. Lasers Eng.*, vol. 38, pp. 1173–1184, 2002.
- [16] E. T. Shimizu, "Directional discrimination in the self-mixing type laser Doppler velocimeter," *Appl. Opt.*, vol. 26, pp. 4541–4544, 1987.
- [17] G. Plantier, N. Servagent, A. Sourice, and T. Bosch, "Real-time parametric estimation of velocity using optical feedback interferometry," *IEEE Trans. Instrum. Meas.*, vol. 50, pp. 915–919, Aug. 2001.
- [18] T. Shibata, S. Shinohara, H. Ikeda, H. Yoshida, T. Sawaki, and H. Sumi, "Laser speckle velocimeter using self-mixing laser diode," *IEEE Trans. Instrum. Meas.*, vol. 45, no. 2, pp. 499–503, Apr. 1996.
- [19] G. Plantier, A. Sourice, T. Bosch, and N. Servagent, "Accurate and real-time doppler frequency estimation with multiplicative noise for velocity measurements using optical feedback interferometry," in *IEEE Sensors Conf.*, 2002, pp. 97–101.
- [20] J. C. Dainty, *Laser Speckle and Related Phenomena*. New York: Springer-Verlag, 1984.

- [21] S. M. Kay, *Modern Spectral Estimation: Theory and Application*. Englewood Cliffs, NJ: Prentice-Hall, 1988.
- [22] —, *Fundamentals of Statistical Signal Processing: Estimation Theory*. Englewood Cliffs, NJ: Prentice-Hall, 1993.
- [23] W. H. Press, S. A. Teukolsky, W. T. Vetterling, and B. P. Flannery, *Numerical Recipes in C: The Art of Scientific Computing*. Cambridge, U.K.: Cambridge Univ. Press, 1992.
- [24] N. Servagent, F. Gouaux, and T. Bosch, "Measurements of displacement using the self-mixing interference in a laser diode," *J Opt.*, vol. 29, no. 3, pp. 168–173, 1998.
- [25] G. Giuliani, S. Bozzi-Pietra, and S. Donati, "Self-mixing laser diode vibrometer," *Meas. Sci. Technol.*, vol. 14, no. 1, pp. 24–32, 2003.
- [26] D. Royer and V. Kmetik, "Measurement of piezoelectric constants using an optical heterodyne interferometer," *Electron. Lett.*, vol. 28, no. 19, pp. 1828–1830, 1992.
- [27] A. L. Kholkin, C.Ch. Wüchrich, D. V. Taylor, and N. Setter, "Interferometric measurements of electric field-induced displacements in piezoelectric thin films," *Rev. Sci. Instrum.*, vol. 67, no. 5, pp. 1935–1941, 1996.
- [28] G. Martini, "Analysis of a single-mode optical fiber piezoceramic phase modulator," *Opt. Quantum Electron.*, vol. 19, pp. 179–190, 1987.

**Lorenzo Scalise** was born in Siena, Italy, in 1971. He received the degree in electronic engineering from the Università di Ancona, Ancona, Italy, in 1993 and the Ph.D. degree in measurement techniques for engineering from the University of Padova, Padova, Italy, in 1999.

He spent nine months in the Biomedical Optics group at the Departments of Applied Physics, Twente University, Twente, The Netherlands. Since 1999, he has been an Assistant Researcher at the Università di Ancona. His research interests include design and development of optical sensors for velocity, displacement and shape measurements, including self-mixing interferometry. He has authored more than fifteen papers in international peer-reviewed journals.

Dr. Scalise has been a member of SPIE since 1999.

**Yanguang Yu** was born in 1964. She received the Ph.D. degree in precision instruments and mechanisms from the Harbin Institute of Technology, Harbin, China, in 2000.

She received the title of Associate Professor from the College of Information Engineering, Zhengzhou University, Zhengzhou, China in 2000. She spent two years for her post doctoral research at the Opto-Electronics Information Science and Technology Laboratory, Tianjin University, China. In 2002, she joined the Optoelectronics Group, Dipartimento di Elettronica, Università di Pavia, Pavia, Italy, as a Visiting Researcher within the ICTP-TRIL program. Her research interests are related to optical feedback in semiconductor lasers and its industrial application, such as measuring vibration, distance, and displacement.

**Guido Giuliani** (M'99) was born in Milan, Italy, in 1969. He received the degree (with honors) in electronic engineering and the Ph.D. degree in electronics and computer science from the Università di Pavia, Pavia, Italy, in 1993 and 1997, respectively.

Since 2000, he has been an Assistant Professor at the Università di Pavia. His research interests include semiconductor lasers, laser diode self-mixing interferometry, optical amplifier noise, semiconductor optical amplifiers, and electrooptical gyroscopes. He has authored more than 15 papers in international peer-reviewed journals.



**Guy Plantier** (M'00) was born in Alès, France, in 1961. He received the title of Engineer from the National School of Engineers of Brest, France, in 1984 and the Ph.D. degree in acoustics from the University of Le Mans, France, in 1991.

He spent two years in the Acoustics and Vibrations Group, Sherbrooke University, Sherbrooke, QC, Canada. In 1993, he joined the Ecole Supérieure d'Electronique de l'Ouest (ESEO), Angers, France, where he is now the Head of the Electronics and Physics Department. He has cooperated in several

R&D programs with French and Canadian companies working on sensors and/or actuators design, motor control, metrology, signal processing, and telecommunications. His research interests are related to signal processing for instrumentation, vibration and velocity measurements, laser Doppler anemometry, active noise control of sounds and vibrations, and communications.



**Thierry Bosch** (M'93) was born in 1965. He received the Ph.D. degree from the National Institute of Applied Science of Toulouse (INSAT), Toulouse, France, in 1992.

In 1993, he joined the Department of Automatic Control and Production Systems, Engineering School of Mines of Nantes, Nantes, France, as an Assistant Professor. He was Head of the Group on Optoelectronics, Instrumentation, and Sensors from 1993 to 2000. He is presently a Professor in the Engineering School ENSEEIHT, Toulouse,

and Director of the Electronics Laboratory, ENSEEIHT (LEN7). He has cooperated in several R&D programs with European companies active in the areas of sensor design, metrology, transportation, or avionics. He has been Guest coeditor for the *Journal of Optics* (June 1998 and November 2002) and *Optical Engineering* (January 2001). With Prof. M. Lescure, he edited the Milestone Volume *SPIE Selected Papers on Laser Distance Measurements* in 1995. He has authored or coauthored more than 20 papers and more than 30 communications in international conferences. He has coauthored about ten industrial contract reports. His research interests are related to laser industrial instrumentation development, including range-finding techniques, vibration, and velocity measurements.

Dr. Bosch is now the Chairman of the IEEE Instrumentation and Measurement Technical Committee Laser and Optical Systems and serves as an Associate Editor of the IEEE TRANSACTIONS ON INSTRUMENTATION AND MEASUREMENT. He has organized several national and international meetings either as a Chairman or a Steering/Program Committee member and he chaired the International Conference ODIMAP in 1997.